

# Representation of a nonspherical ice particle by a collection of independent spheres for scattering and absorption of radiation

Thomas C. Grenfell and Stephen G. Warren

Department of Atmospheric Sciences, University of Washington, Seattle

**Abstract.** The use of “equivalent” spheres to represent the scattering and absorption properties of nonspherical particles has been unsatisfactory in the past because the sphere of equal volume has too little surface area and thus too little scattering, whereas the sphere of equal area has too much volume giving too much absorption. Their asymmetry factors are also too large. These problems can largely be avoided if the real cloud of nonspherical particles is represented by a model cloud of spheres where the model cloud contains the same total surface area as well as the same total volume. Each nonspherical particle is then represented not by just one sphere but rather by a collection of independent spheres that has the same volume-to-surface-area (V/A) ratio as the nonspherical particle. To demonstrate the broad utility of this approach, we show results for ice, whose absorption coefficient varies with wavelength by 8 orders of magnitude. Randomly oriented infinitely long circular cylinders are used as a test case because an exact solution is available for all size parameters. The extinction efficiency and single-scattering albedo are closely approximated by the values for equal-V/A spheres across the ultraviolet, visible, and infrared from 0.2 to 50  $\mu\text{m}$  wavelength; the asymmetry factor is matched somewhat less well. Errors in hemispheric reflectance, absorptance, and transmittance are calculated for horizontally homogeneous clouds which cover the range of crystal sizes and optical depths from polar stratospheric clouds through cirrus clouds to surface snow. The errors are less than 0.05 at all wavelengths over most of this space.

## 1. Introduction

Because of the importance of ice clouds and surface snow for the Earth's climate, it is desirable to find efficient yet accurate ways to represent the scattering and absorption properties of ice crystals in radiation models and climate models. Models commonly use “equivalent spheres” to represent nonspherical particles because of their ease of use and the saving in computation time. This saving can be several orders of magnitude.

A variety of crystal shapes is observed in natural ice clouds and snow packs. Figure 1 shows some examples of “diamond dust” atmospheric ice crystals collected as they fell over the Antarctic Ice Sheet. In some cases, length-to-width ratios can be very large (Figure 1b).

It is popular to classify an ice crystal by either its volume  $V$  or its surface area  $A$ . However, both the sphere of equal volume, whose radius is  $r_V$ , and the sphere of equal surface area, with radius  $r_A$ , have single-scattering albedos ( $\omega_0$ ) which are too small and asymmetry factors ( $g$ ) which are too large. This is also true if equal projected area is used instead of equal surface area to define the equal-area sphere. Radiative transfer predictions using either equal-volume spheres or equal-area spheres will therefore be in error. Scattering efficiencies and phase functions have been calculated for hexagonal columns and plates of ice and

compared to equal-area or equal-volume spheres by *Takano and Liou* [1989] and *Chylek and Videen* [1994]. The most thorough criticism of equivalent spheres was presented by *Liou and Takano* [1994], who compared phase functions, asymmetry factors, effects on remote sensing, spectral and broadband albedos, and cloud radiative forcing by cirrus clouds, concluding in all instances that the use of equivalent spheres in models leads to large errors. In spite of their inadequacy shown in those studies, prescriptions of equivalent spheres as those of equal surface area (or projected area), or equal volume, are still commonly used. For example, *Ebert and Curry* [1992] used equal-area spheres in their parameterization of ice cloud optical properties for climate models.

Some attempts [e.g., *Sun and Shine*, 1995] have been made to “adjust” the results of Mie calculations for spheres to match those of nonspherical particles. *Schmidt et al.* [1995] proposed a “composite” sphere to which is assigned a phase function appropriate to hexagonal crystals. Such ad hoc adjustments can be made for specific applications, but they fail to work in general. We seek instead a general method that can work for all shapes, all sizes, all wavelengths, all chemical compositions, and all optical depths.

We investigate here the possibility that a third choice of equivalent sphere can more accurately mimic the single-scattering properties and, more importantly, the multiple-scattering properties of nonspherical particles in the ultraviolet, visible, and infrared spectral regions. In our view, the reason for the failure of equivalent spheres to adequately represent nonspherical particles in the studies cited above is the requirement that the number of spheres  $n_s$  must equal the

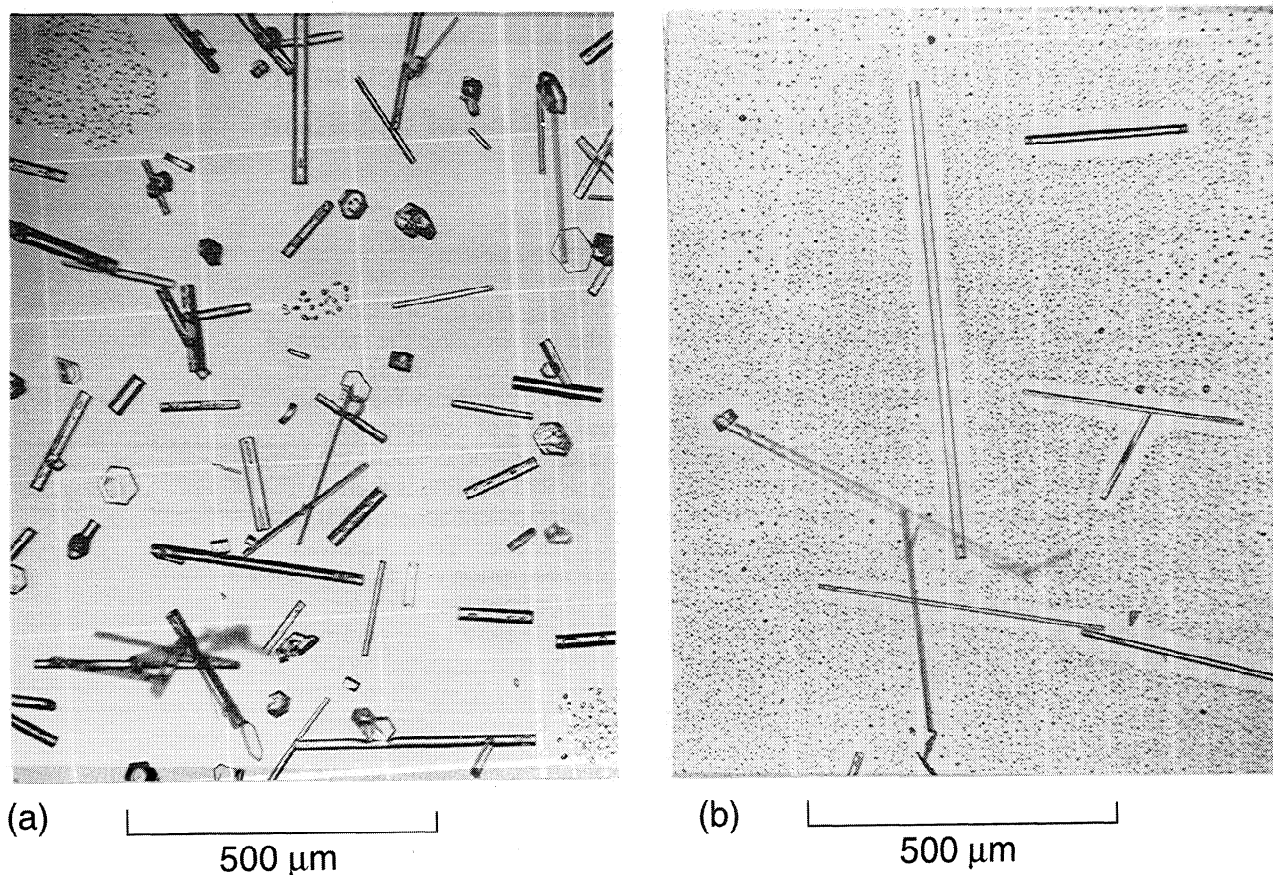


**Figure 1.** Photographs of atmospheric hexagonal ice crystals ("diamond dust") collected at Amundsen-Scott South Pole Station as they fell during the austral winter of 1992 are shown in Figure 1a. The long needles shown in Figure 1b, called Shimizu crystals [Shimizu, 1963], have an aspect ratio of approximately 50:1.

number of nonspherical particles  $n$ . We show that a significant benefit can be obtained by relaxing that requirement.

## 2. Approach

To model the radiative properties of an ice particle in a cloud or a snowpack, we represent the single particle by a collection of monodisperse spheres which contains the same total surface area as the original particle as well as the same total volume of ice. These spheres, whose radius is  $r_{VA}$ , then have the same volume-to-surface ratio as the nonspherical particle, but in order to conserve the total mass there is more than one sphere for each nonspherical particle. For radiative transfer there is no compelling reason why the number of particles in the model cloud should be the same as the number in the real cloud. In the case of snow, where the particles are in contact, there is even less reason, as it is often arbitrary to say where one snow grain ends and another begins. We therefore have abandoned the conventional requirement that  $n_s = n$ .

The arguments in favor of taking account of the volume-to-surface ratio have a long history. In arguing for the use of equal-V/A spheres to represent snow particles, Wiscombe and Warren [1980] and Warren [1982] cited Pollack and Cuzzi's [1980] work on aerosol particles. Mitchell and Arnott [1994] pointed out that the importance of the V/A ratio had been

mentioned even earlier by Bryant and Latimer [1969]. The representation of a snow grain by a collection of equal-V/A spheres was further discussed by Grenfell *et al.* [1994]. Wiscombe and Warren's [1980] recommendation of equal-V/A spheres was adopted in the snow-optics community, where some empirical evidence for it was found in attempts to match measured and calculated reflectance [Grenfell *et al.*, 1981; Dozier, 1989]. In the context of cirrus clouds, equal-V/A spheres were recommended by Foot [1988], who also cited Pollack and Cuzzi [1980] for inspiration, but these smaller spheres have been slower to gain acceptance in the cloud-optics community than was the case for snow.

There are reasons to expect equal-V/A spheres to do better than the equal-area spheres or equal-volume spheres at mimicking the radiative properties of real clouds. It was mentioned above that equal-area spheres and equal-volume spheres have  $\omega_0$  too small and  $g$  too large. Both errors would be reduced by using equal-V/A spheres because they are smaller, as smaller spheres have larger  $\omega_0$  and smaller  $g$ . The nonspherical ice crystals sampled in clouds during the FIRE-cirrus experiment in Wisconsin were converted to equal-volume or equal-area spheres, which turned out to be too large to explain the radiation measurements [Platt *et al.*, 1989; Wielicki *et al.*, 1990; Ackerman *et al.*, 1990; Heymsfield *et al.*, 1990; Sassen *et al.*, 1990].

Equal-V/A spheres might reduce the discrepancies seen in

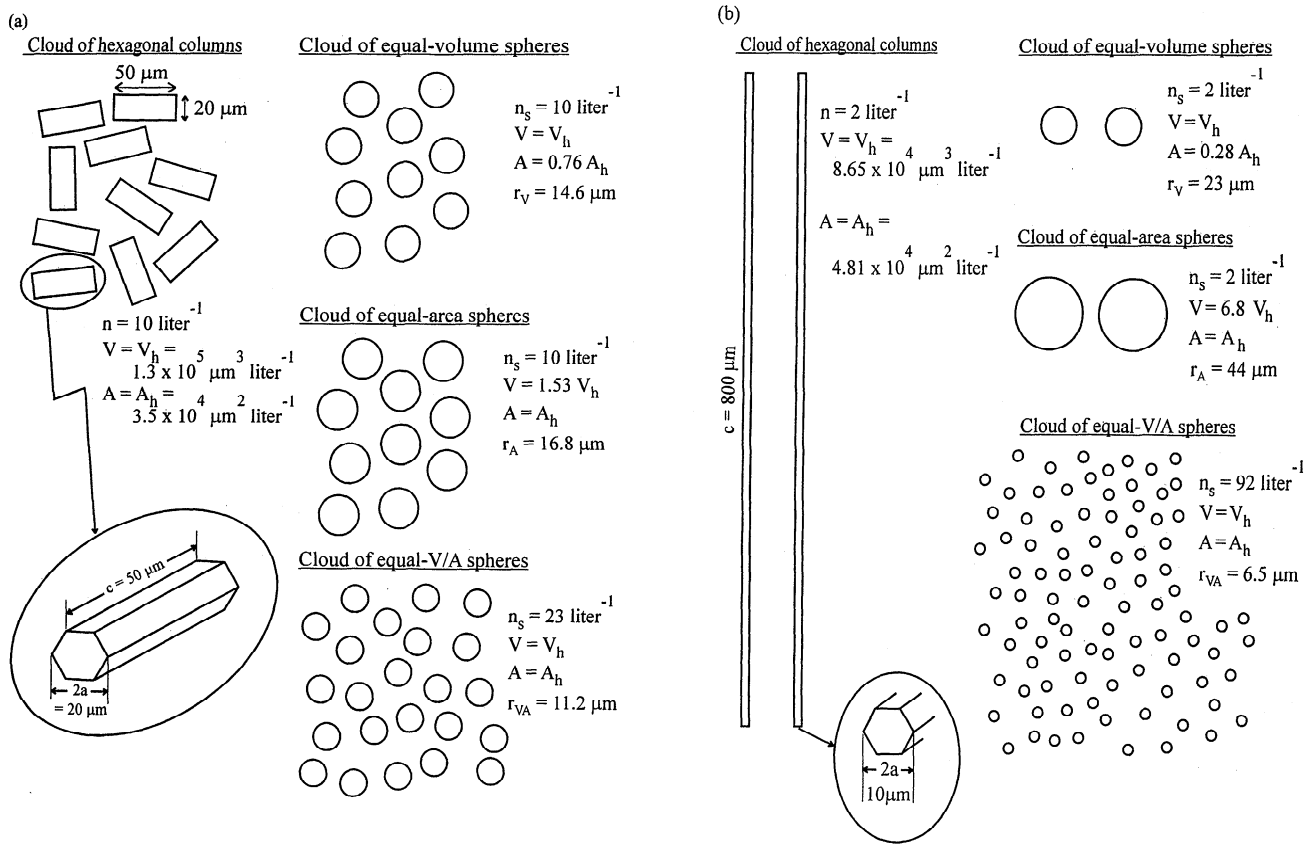


**Figure 2.** Hexagonal columns represented as spheres of equal volume, equal surface area, and equal V/A. In Figure 2a, the crystal dimensions are  $20 \times 50 \mu\text{m}$ , and in Figure 2b they are  $10 \times 800 \mu\text{m}$ .

FIRE. A step in this direction was taken by Kinne *et al.* [1990, Figure 2], who modeled the individual elements of a cluster as separate spheres. A prescription for effective radius proposed by Fu [1996] and Fu *et al.* [1998] makes use of the equal-V/A principle. Mitchell and Arnott [1994] pointed out that the single-scattering albedo was too small for equal-projected-area spheres and argued for use of a measure of volume-to-surface ratio. The idea was further developed by Mitchell *et al.* [1996], who defined the “effective distance”  $d_e$  as the representative distance a photon travels through ice between opportunities for reflection or refraction and then calculated  $d_e$  for different shapes of ice crystals. Such calculations have also been made by Wyser and Yang (1998). Recently, McFarquhar and Heymsfield [1998] have reviewed these and the other specifications that have been used for effective radius for ice clouds. Among them, the methods of Fu and Mitchell and their coworkers are the closest to what we propose but are more complicated. The prescription pursued in this paper, if successful, offers in addition the advantage of simplicity.

### 3. Formulation

We wish to represent a particle of volume  $V$  and surface area  $A$  by a collection of spheres. Since the ratio  $V/A$  for a sphere is equal to  $r/3$ , we obtain the radius of the equal-V/A sphere from the relation

$$r_{VA} = 3 \frac{V}{A}. \quad (1)$$

The number of equivalent spheres  $n_s$  relative to the number of nonspherical particles  $n$  is given by

$$\frac{n_s}{n} = \frac{3V}{4\pi r_{VA}^3}. \quad (2)$$

For hexagonal columns, with dimensions  $a$  and  $c$ , as shown in Figure 2, the spherical radii for the three different specifications are given by

$$r_{VA} = \frac{3\sqrt{3}ac}{4c + 2\sqrt{3}a}$$

$$r_A = \left[ \frac{6ac + 3\sqrt{3}a^2}{4\pi} \right]^{1/2} \quad (3)$$

$$r_V = \left[ \frac{9\sqrt{3}a^2c}{8\pi} \right]^{1/3}.$$

The same result is obtained if projected area,  $P$ , rather than total surface area,  $A$ , is used to describe the particles because their ratio is constant ( $A = 4P$ ) for all convex shapes when randomly oriented (Vouk, 1948). If equal-V/A spheres are used, the value of  $n_s$  is then determined from (2) using

$$V = \frac{3\sqrt{3}a^2c}{2}. \quad (4)$$

In general,  $r_A > r_V > r_{VA}$ . For example, short hexagonal columns of length  $50 \mu\text{m}$  and width  $20 \mu\text{m}$ , shown in Figure 2a, give  $r_A = 17 \mu\text{m}$ ,  $r_V = 15 \mu\text{m}$ ,  $r_{VA} = 11 \mu\text{m}$ , and  $n_s/n = 2.3$ . In the case of the very long narrow columns in Figure 2b, a single column is represented by 46 small spheres in the equal-V/A representation.

For the computation of  $r_{VA}$  to represent hollow crystals,  $V$  is just the volume of ice alone, not including the air pockets. The appropriate area is probably the total surface area including both interior and exterior walls, unless they are perfectly parallel. However, hollow crystals are not considered in this paper.

In this initial study, the nonspherical shape we use is not a hexagonal column nor a hexagonal plate but rather an infinitely long circular cylinder. The reason for using infinite circular cylinders in this initial demonstration project is that an exact solution is available. This allows us to determine the errors in the radiation fields, due to representing the cylinders by spheres, for any size parameter and any value of the complex index of refraction. For infinite circular cylinders, with radius  $r_{cyl}$ , the radii for the three different specifications of equivalent spheres are

$$r_{VA} = 1.5 r_{cyl} \quad r_A = \infty \quad r_V = \infty. \quad (5)$$

#### 4. Single Scattering

The scattering properties for spheres were calculated from Mie theory [Wiscombe, 1979; 1980] and for cylinders from a corresponding solution of Maxwell's equations [Kerker, 1969; Bohren and Huffman, 1983; Haracz et al., 1985] which yield the extinction efficiency  $Q_{ext}$ , the single scattering albedo  $\omega_s$ , and the phase function  $p(\Theta)$ . The complex re-

fractive index of ice was obtained principally from measurements by Grenfell and Perovich [1981] for the wavelength range  $0.4$  to  $1.4 \mu\text{m}$  and by Schaaf and Williams [1973] for  $2.8$  to  $33 \mu\text{m}$ , as reviewed by Warren [1984]. Warren's [1984] compilation is used here, with updates from Perovich and Govoni [1991] in the near ultraviolet and from Kou et al. [1993] from  $1.4$  to  $2.8 \mu\text{m}$ . (The updated compilation is available by anonymous FTP to climate.gsfc.nasa.gov in the file /pub/wiscombe/Refrac\_Index/ICE.) The calculations for randomly oriented infinite cylinders, using the method of Haracz et al. [1985], were carried out using a slightly modified version of computer code provided to us by B.T.N. Evans (Department of National Defense, Defense Research Establishment Ottawa, Canada, e-mail bevans@airsrv.abdr.dreo.dnd.ca).

To average over the resonant peaks in the phase functions, the single scattering computations were performed for a lognormal distribution of particle sizes with a specified geometric mean radius  $r_g$  and a fixed geometric standard deviation  $\sigma_g = 1.6$ . This value of  $\sigma_g$  corresponds to that typically obtained for the size distributions (when converted to equal-V/A spheres) which we measured in photographs of falling ice crystals collected on 100 days in the winter of 1992 at the South Pole, two of which are shown in Figure 1. The resulting size distributions for the infinite cylinders are shown in Figure 3. Calculations were done with mean cylinder radii of  $r_g = 1, 2, 5, 10, 20, 50, 100, 200,$  and  $500 \mu\text{m}$ . For radiative purposes the most useful single number to characterize a size distribution is the area-weighted mean radius, or "effective radius,"  $r_{eff}$  [Hansen and Travis, 1974]:

$$r_{eff} = \frac{\int r^3 n(r) dr}{\int r^2 n(r) dr}. \quad (6)$$

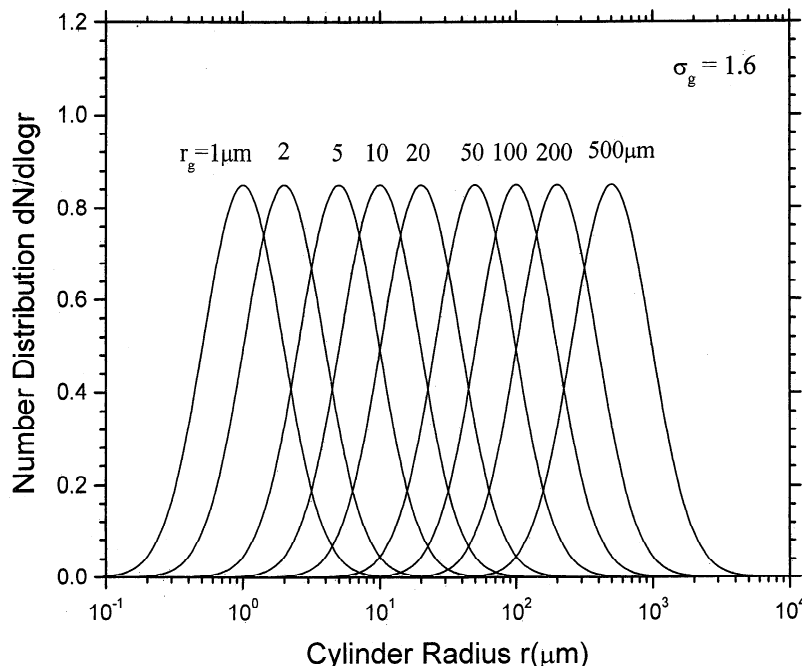


**Figure 3.** Lognormal distributions for the radii of infinite circular cylinders used in the modeling, where  $N$  is the integrated number density between zero and  $r$ . The geometric standard deviation  $\sigma_g$  is 1.6 for all cases. The geometric mean radius is  $r_g$ .

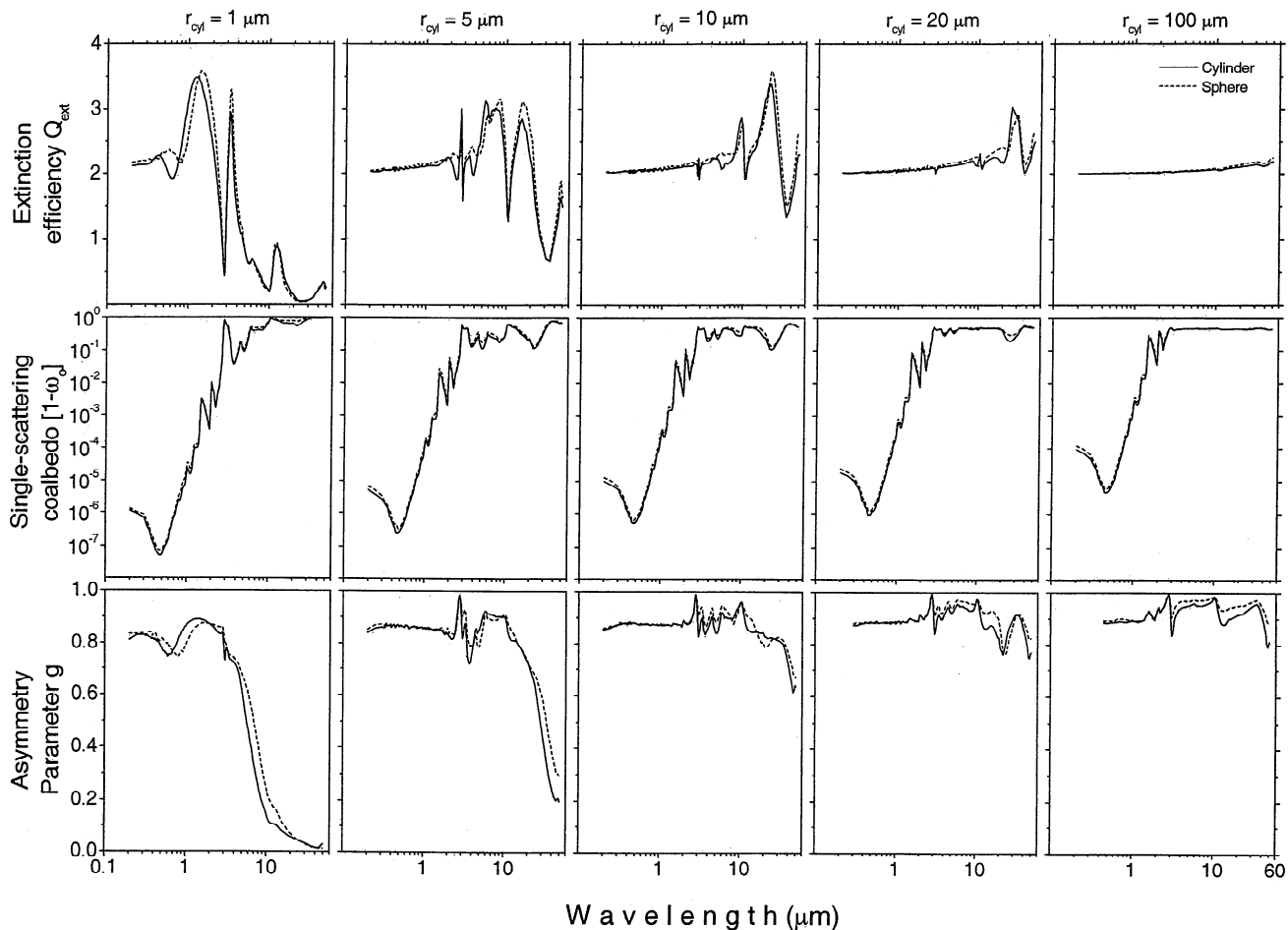


**Figure 4.** Extinction efficiency ( $Q_{ext}$ ), single-scattering coalbedo ( $1-\omega_0$ ), and asymmetry parameter ( $g$ ) versus wavelength from 0.2 to 50  $\mu\text{m}$  for randomly oriented infinite circular cylinders (solid lines) and equal-V/A spheres (dashed lines). The geometric mean radii for the cylinder size distributions are indicated at the top of each column.

For a lognormal distribution,  $r_{eff}$  is given by

$$r_{eff} = r_g \exp[2.5 (\ln \sigma_g)^2]. \quad (7)$$

For  $\sigma_g = 1.6$ , we obtain  $r_{eff} = 1.737 r_g$ . In the discussions throughout the rest of the paper, size distributions are identified by the value of  $r_g$  specified.

The phase function was computed at an angular sampling density selected so that 20 points were used between zero scattering angle and the first minimum in the diffraction pattern. Values of the first four moments of the phase function were then calculated numerically to be used in the radiative transfer model.

Examples of the single-scattering results for randomly oriented cylinders are shown in Figure 4 for cylinder radii ( $r_g$ ) of 1, 5, 10, 20, and 100  $\mu\text{m}$  for wavelengths ( $\lambda$ ) from 0.2  $\mu\text{m}$  to 50  $\mu\text{m}$ . This covers essentially the entire solar shortwave and terrestrial longwave spectral regions. The extinction efficiency and single-scattering coalbedo of the cylinders are closely approximated by the values for spheres with the same V/A ratio. The asymmetry factor is too large in some spectral regions and too small in others depending on cylinder radius, but the effects of these errors on irradiances and heating rates are usually small, as shown in section 5.

Phase functions for representative cases of 5  $\mu\text{m}$  and 20  $\mu\text{m}$  cylinders are shown in Figure 5. Although the asymmetry factors are in close agreement, the forward peak of the phase function for spheres is always stronger than that for the cylinders. This is because the forward scattering diffraction maximum for the spheres is proportional to the fourth power of the size parameter ( $x = 2\pi r/\lambda$ ), while for the infinite cylinders, it is proportional to  $x^2$ . The reduced side scattering of spheres ( $\Theta \approx 90^\circ$ ) relative to that of nonspherical particles is well known from other studies [Liou, 1973, Figure 1; Wendling et al., 1979, Figure 8; Mishchenko et al., 1996, Figure 1]. We shall see, however, that these differences in the phase functions lead to little error in radiation fluxes.

## 5. Multiple Scattering

We now compare the bulk radiative properties of a horizontally homogeneous cloud of randomly oriented infinite circular cylinders to those of a cloud of equal-V/A spheres. Calculations of hemispherical reflectance, absorptance, and transmittance were carried out for wavelengths 0.2-50  $\mu\text{m}$  using a four-stream delta-M discrete-ordinates method [Grenfell, 1991]. To isolate the inherent properties of the

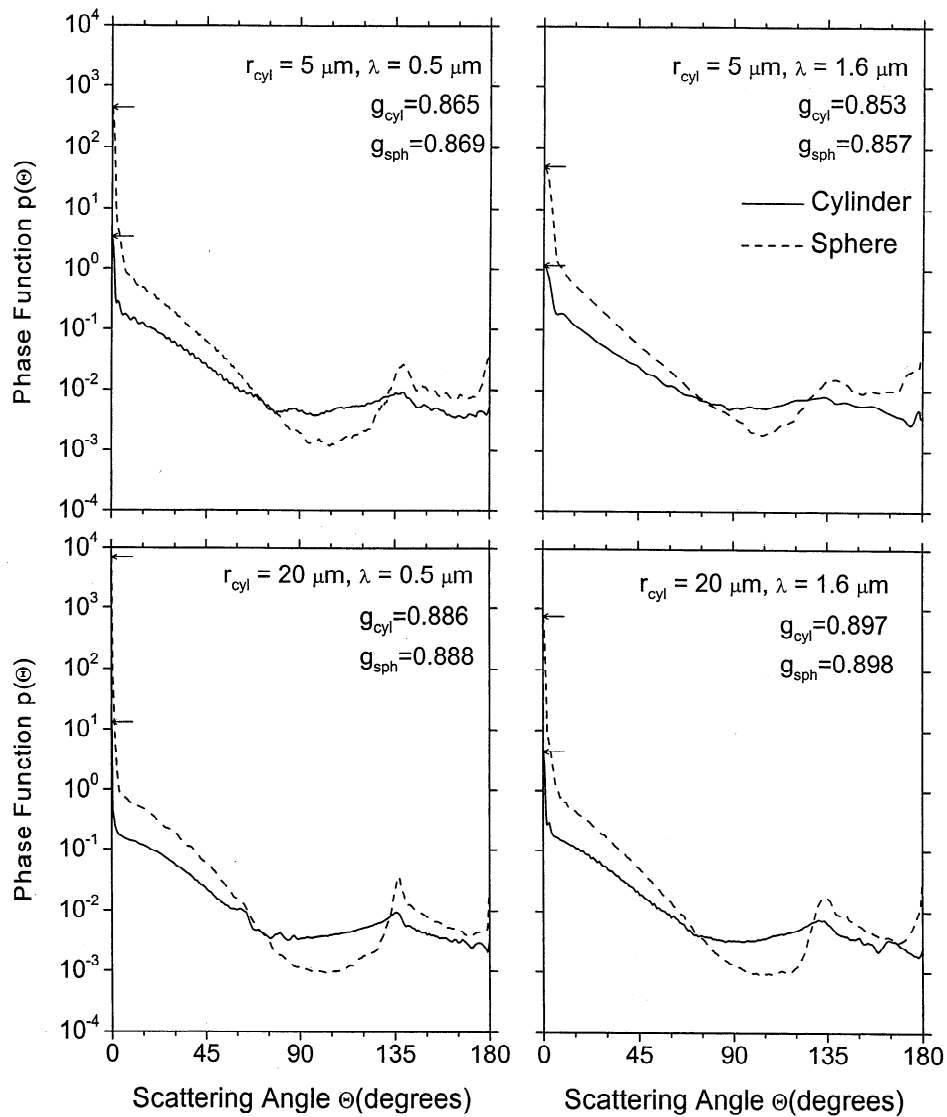


**Figure 5.** Phase functions  $p(\Theta)$  for cylinders (solid lines) with mean radii of 5 and 20  $\mu\text{m}$  at wavelengths of 0.5 and 1.6  $\mu\text{m}$  (solid lines) compared to those of equal-V/A spheres (dashed lines). The corresponding asymmetry factors are given in each frame. The arrows pointing to the phase-function axis indicate the values of  $p(\Theta)$  at  $\Theta = 0^\circ$ .

cloud itself, the model consisted of a single homogeneous cloud layer over a black surface at  $0^\circ\text{K}$  illuminated from above by a plane wave at a zenith angle of  $60^\circ$ . In the thermal infrared the absorptance can be equated to the directional emissivity at an emission angle of  $60^\circ$ . It is useful to express the optical properties of a cloud as functions of the ice water path (IWP), defined as the total mass per unit area, integrated vertically through the cloud. The relation of IWP to optical depth  $\tau$  is given by formulas similar to that derived by Stephens [1978] for liquid clouds. For a monodispersion, the differential of optical depth  $d\tau$  is given by

$$d\tau = Q_{ext}(r) A_p(r) n(r, z) dz, \quad (8)$$

where  $A_p(r)$  is the angular averaged projected area of a single particle (sphere or cylinder) of radius  $r$  and  $n(r, z)$  is the number density of particles. The mass of ice per unit volume of the cloud (the ice water content IWC) is given by

$$\text{IWC}(z) = V(r) n(r, z) \rho_{ice}, \quad (9)$$

where  $V(r)$  is the volume per particle and  $\rho_{ice}$ , the density of pure ice, is  $916 \text{ kg/m}^3$ . Combining (9) and (8) gives

$$d\tau = \frac{A_p(r) Q_{ext}(r)}{V(r) \rho_{ice}} \text{IWC}(z) dz. \quad (10)$$

For a monodispersion, integrating over  $z$  gives

$$\tau = \frac{A_p(r) Q_{ext}(r)}{V(r) \rho_{ice}} \text{IWP}. \quad (11)$$

For a cloud of spheres  $A_p/V = 3/(4r)$ , so

$$\tau_{sph} = \frac{3 \text{IWP} Q_{ext}(r_{sph})}{4 r_{sph} \rho_{ice}}. \quad (12)$$

For a cloud of randomly oriented cylinders we have

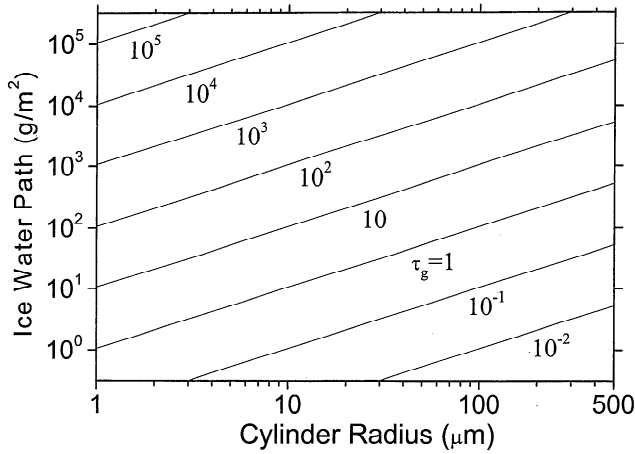


**Figure 6.** Contours of constant optical depth ( $\tau_g$ ) in the geometric-optics limit ( $Q_{ext} = 2$ ) for the ranges of ice water path and cylinder radius shown in Figures 7-9.

$$\frac{\langle A_{cyl} \rangle}{V_{cyl}} = \frac{2r \int_0^{\pi/2} \sin^2 \theta d\theta}{\pi r^2 \int_0^{\pi/2} \sin \theta d\theta} = \frac{1}{2r_{cyl}}, \quad (13)$$

giving

$$\tau_{cyl} = \frac{1}{2} \frac{IWP Q_{ext}(r_{cyl})}{r_{cyl} \rho_{ice}}. \quad (14)$$

From Equation (1) we find that  $r_{sph} = 1.5 r_{cyl}$ , so for a given IWP and  $Q_{ext}$  we have

$$\frac{\tau_{sph}}{\tau_{cyl}} = \frac{Q_{ext}(r_{sph})}{Q_{ext}(r_{cyl})}. \quad (15)$$

Figure 4 shows that  $Q_{ext}(r_{cyl}) \approx Q_{ext}(r_{sph})$ , so

$$\tau_{sph} \approx \tau_{cyl}. \quad (16)$$

Equation (15) was derived for a monodispersion. It is therefore valid for all components of a polydispersion and therefore must be valid for the polydispersion itself.

The inherent optical properties of the cloud are thus specified by IWP,  $r_{cyl}$ , and the single scattering quantities. Our calculations were carried out for the nine size distributions of cylinder radii shown in Figure 3 and for IWP values ranging from 0.4 to 200,000  $\text{g m}^{-2}$ . These ranges are sufficient to cover the range of crystal sizes and ice water paths from polar stratospheric clouds through surface snowpacks. Approximate optical depths implied by all combinations of IWP and  $r_{cyl}$  are shown in Figure 6. The optical depth depends on wavelength, because  $Q_{ext}$  depends on wavelength, so for Figure 6, we have simply used the geometric optics limit,  $Q_{ext} = 2$ , to plot the "geometric-optics" optical depth  $\tau_g$ .

Representative results for reflectance, absorptance, and transmittance, together with the differences between the exact solution and the equivalent-sphere results, are shown in Figures 7-9 for the particular wavelengths 0.5, 1.6, 3.73, 11, and 24.6  $\mu\text{m}$ . Reflectance is defined as the ratio of upwelling irradiance above the cloud to the incident irradiance.

Absorptance and transmittance are ratios of absorbed and transmitted irradiance to incident irradiance.

The results shown in Figures 7-9 include a very large range in optical depth, from approximately  $10^{-3}$  to  $2 \times 10^5$ , implying reflectance of essentially zero for the smallest optical depths, up to reflectance saturation and zero transmittance for the largest optical depths. The errors in all three quantities are less than 0.02 over much of the three-dimensional space of  $\lambda$ ,  $r_{cyl}$ , and IWP and less than 0.05 over most of the space. The maximum errors are 0.07 for reflectance, 0.09 for absorptance, and 0.07 for transmittance; these largest errors all occur at  $\lambda = 3.73 \mu\text{m}$  and only at particular values of radius and IWP. In some spectral regions a substantial error in single scattering leads to negligible error in multiple-scattering results. For example, Figure 4 shows substantial error in  $g$  at  $\lambda = 11 \mu\text{m}$  for cylinder radii of 20  $\mu\text{m}$  and 100  $\mu\text{m}$  ( $g_{cyl} \approx 0.88$ ;  $g_{sph} \approx 0.93$ ). However, Figures 7-9 show negligible error in reflectance, absorptance, or transmittance for these particle sizes at this wavelength. That is because most incident photons are absorbed at this wavelength, so the phase function is of little importance.

## 6. Discussion

### 6.1. Broad Size Distributions

To test how well the method works for broader size distributions we combined the results from groups of results presented above. The first group was a combination of results for the 5, 10, and 20  $\mu\text{m}$  lognormal distributions shown in Figure 3. The combination weights  $n_i$  of the three categories were taken to be 32, 16, and 1, respectively, giving the same effective radius as that of the 10  $\mu\text{m}$  narrow distribution in Figure 3. The second case combined the results from 20, 50, and 100  $\mu\text{m}$  distributions, using  $n_i$  values of 42, 13, and 1 for the three sizes, giving the same effective radius as that of the 50  $\mu\text{m}$  narrow distribution. Comparison of the combined results (Figure 10) with those presented in Figure 4 shows even better agreement between equivalent spheres and infinite cylinders for the broad size distributions than for the narrow ones. This is due to incoherence among the errors for the different component distributions, which average out to some degree when they are combined.

### 6.2. Application to Realistic Ice-Crystal Shapes

We have shown that equal-V/A spheres can be used to compute quite accurate values of angular-averaged reflectance, transmittance, and absorptance for a multiple-scattering medium. The ability of spheres to represent radiative properties of circular cylinders encourages us to believe that they may do comparably well at mimicking multiple scattering by hexagonal columns and plates. Comparisons such as those shown in this paper will need to be done over the full range of  $r_{VA}$ , IWP, and  $\lambda$  we have used but with the additional variable of axial ratio  $a/c$ . The phase function (Figure 5) is poorly represented by spheres, so spheres cannot be expected to produce accurate radiances at specific angles, particularly if halos are prominent. We are thus promoting the use of spheres for fluxes rather than radiances.

We feel that the representation using equal-V/A spheres may also be suitable for hollow crystals, where the value of V

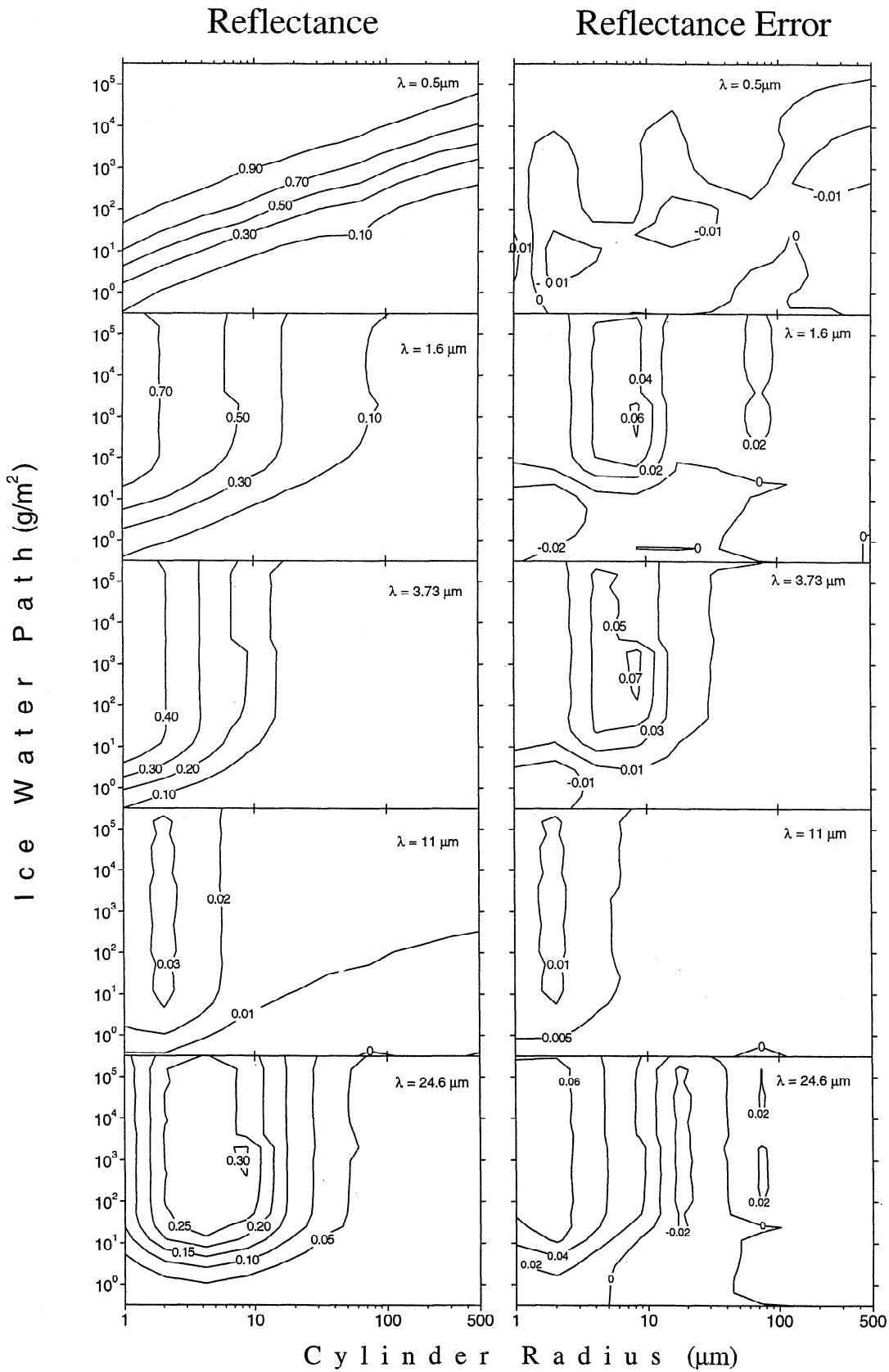


**Figure 7.** Contours of reflectance of ice clouds, and of the errors introduced by the use of equal-V/A spheres to represent ice cylinders, as functions of ice water path and cylinder radius, calculated at the five different wavelengths ( $\lambda$ ) specified in the each of the panels. The cylinder radius specified on the horizontal axis is the geometric mean radius  $r_g$  of a lognormal distribution. The corresponding effective radius (equation (7)) is  $r_{eff} = 1.737 r_g$ . The error plotted is the true cylinder reflectance minus the approximate reflectance using spheres.

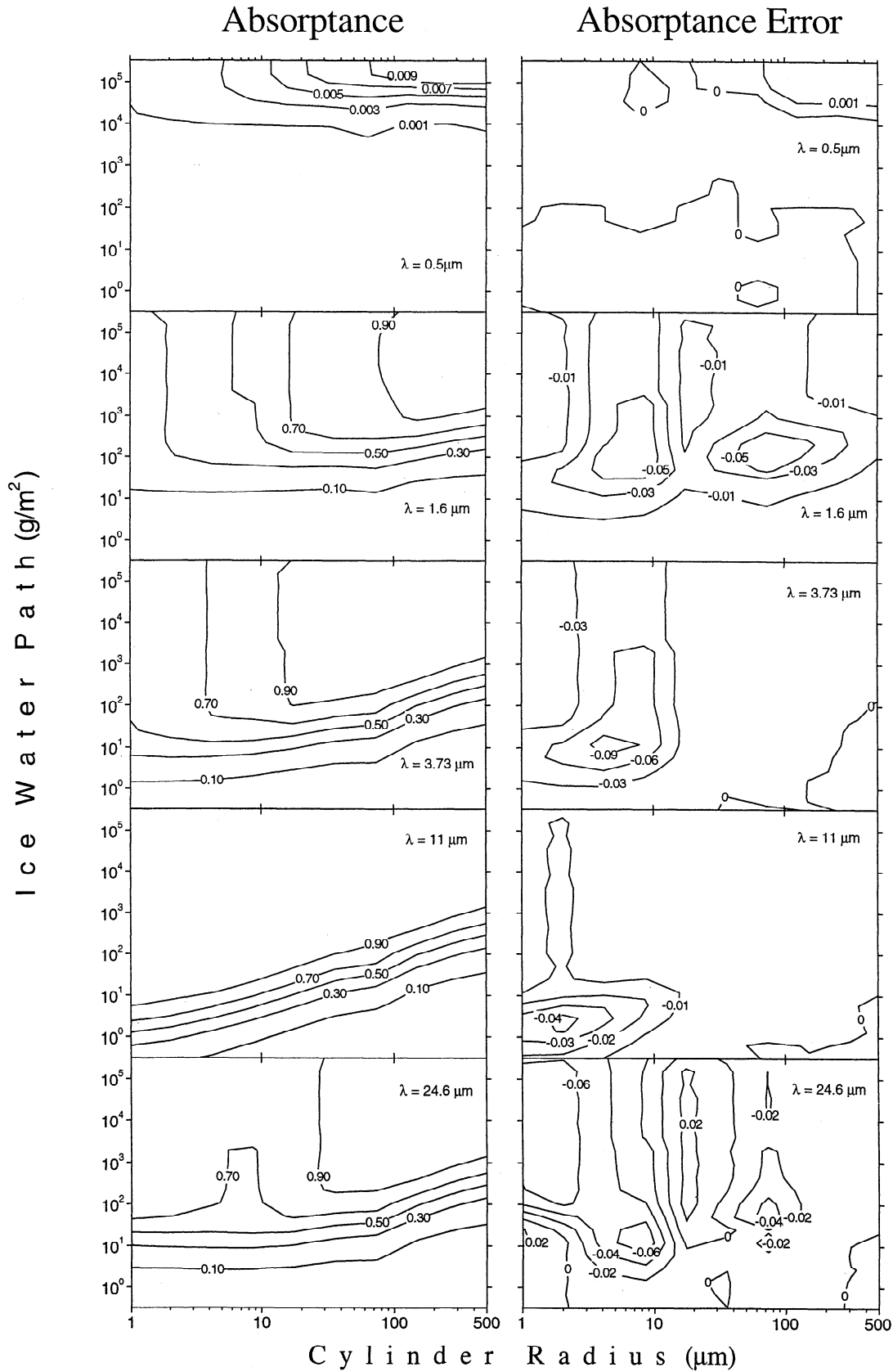


**Figure 8.** Contours of absorptance of ice clouds, and of the errors introduced by the use of equal-V/A spheres to represent ice cylinders, as functions of ice water path and cylinder radius, calculated at the five different wavelengths ( $\lambda$ ) specified in the each of the panels. The error plotted is the true cylinder absorptance minus the approximate absorptance using spheres.

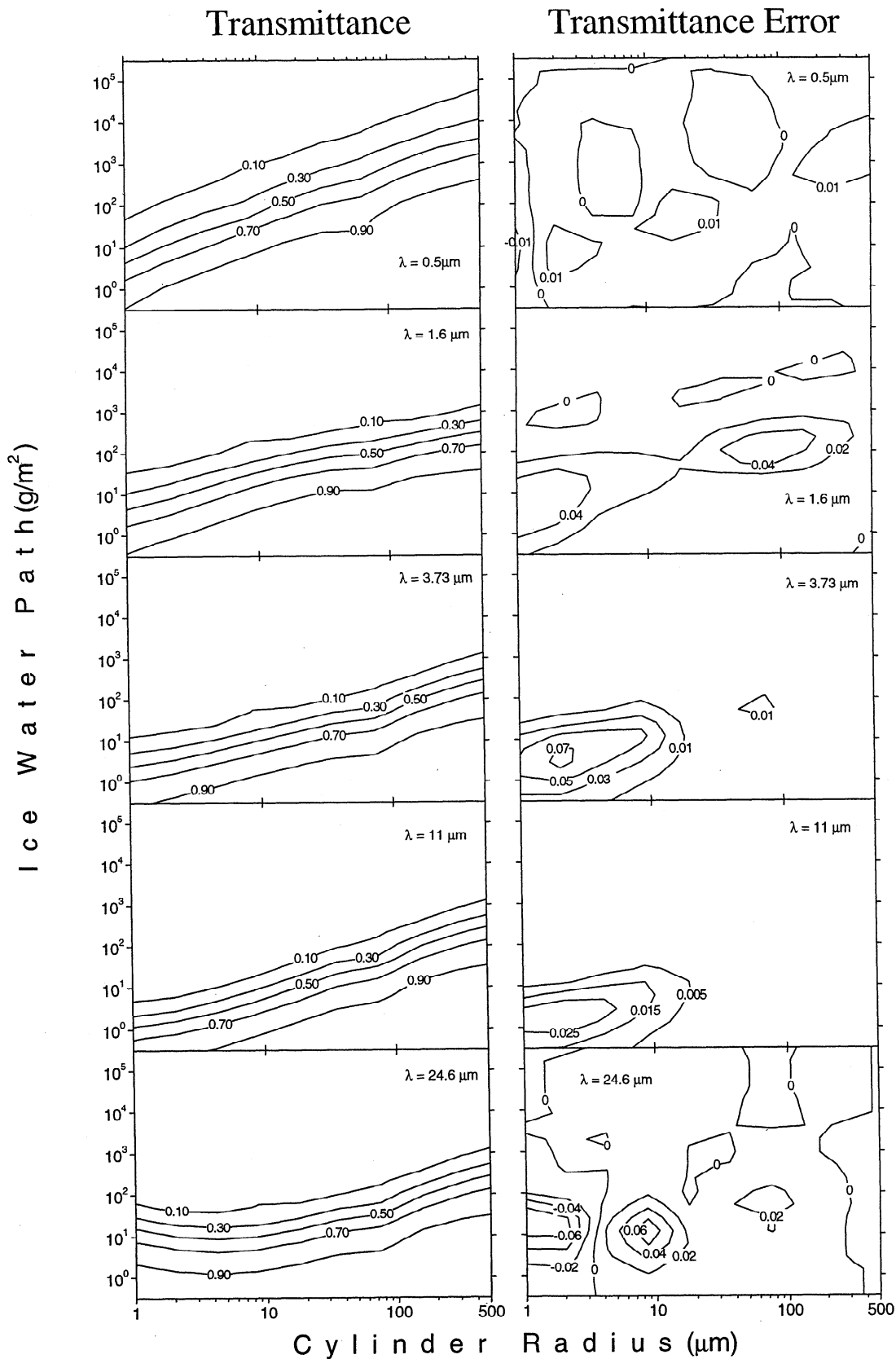


**Figure 9.** Contours of transmittance of ice clouds, and of the errors introduced by the use of equal-V/A spheres to represent ice cylinders, as functions of ice water path and cylinder radius, calculated at the five different wavelengths ( $\lambda$ ) specified in the each of the panels. The error plotted is the true cylinder transmittance minus the approximate transmittance using spheres.

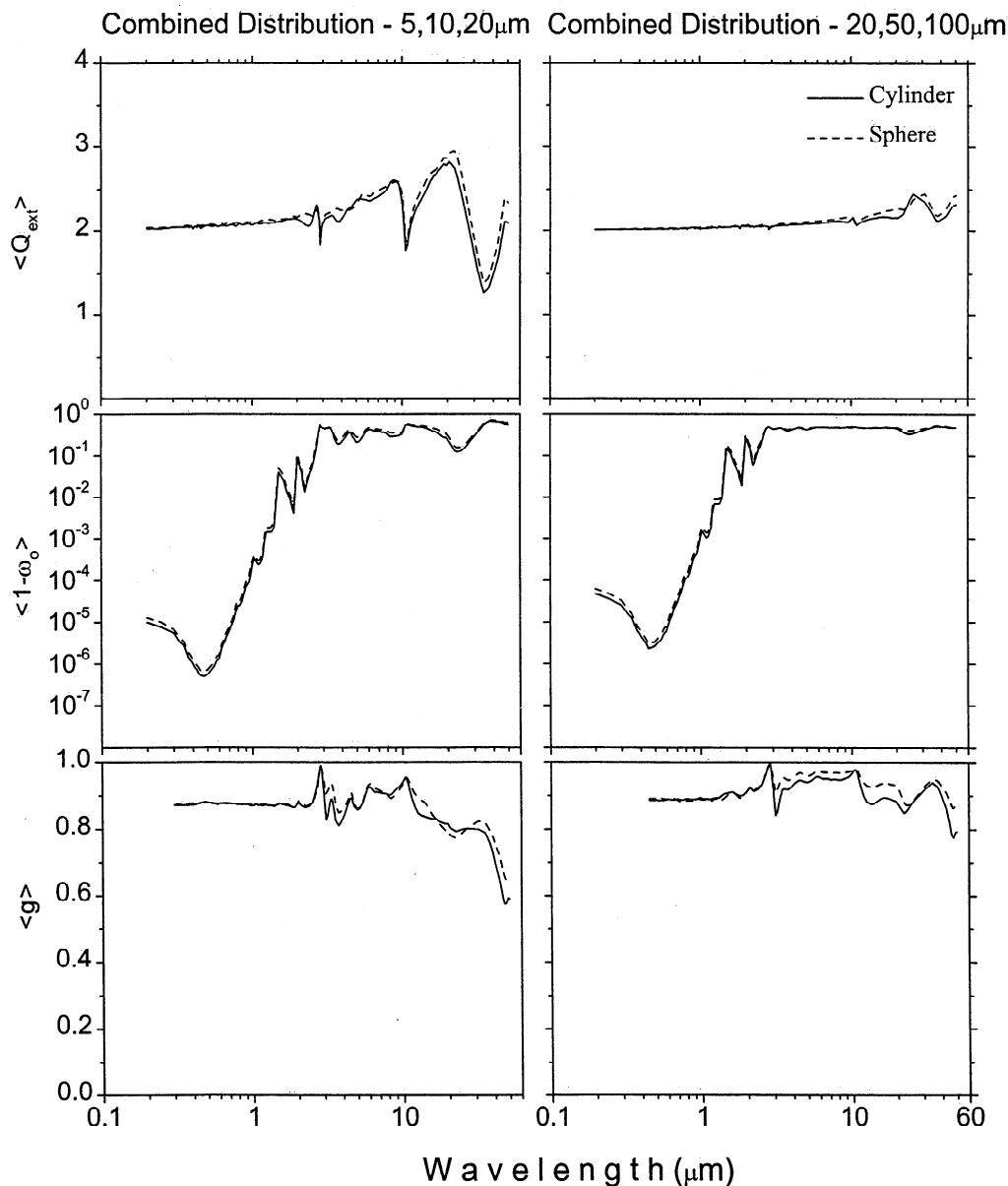


**Figure 10.** Spectral extinction efficiency ( $Q_{ext}$ ), single-scattering coalbedo ( $1-\omega_0$ ), and asymmetry factor  $g$  for broad size distributions of cylinders, and for the corresponding equal-V/A spheres. A broad distribution is made by combining the values for the narrow distributions with mean cylinder radii 5, 10, and 20  $\mu\text{m}$  (left panels), or 20, 50, and 100  $\mu\text{m}$  (right panels), in ratios that cause the effective radius of the broad distribution to be the same as that of the 10  $\mu\text{m}$  or 50  $\mu\text{m}$  narrow distribution. Results for infinite cylinders are given by the solid lines and for spheres by the dashed lines.

is the volume occupied by ice and  $A$  is the total area of both internal and external surfaces. In this and other cases where crystals contain concavities, the projected area is not related to total surface area by a simple multiplier. Consequently, we prefer to use the actual surface area in our prescription for  $r_{VA}$ .

### 6.3. Application to Remote Sensing

Ice crystals in the near-surface atmosphere at the South Pole were collected on gridded slides daily for three months in 1992; two examples are shown in Figure 1. Dimensions of all crystals on each photograph were measured, and the radius of the equivalent sphere computed for each assemblage of

crystals, using three different prescriptions ( $r_A$ ,  $r_V$ ,  $r_{VA}$ ). Effective radii were also inferred for the clouds by a ground-based remote sensing method, using emitted infrared spectral radiances measured at nearly the same time, by Mahesh *et al.* (Ground-based infrared remote sensing of cloud properties over the Antarctic Plateau, II, submitted to Journal of Applied Meteorology, 1999). Their Figure 15 shows that the remotely sensed radii were much smaller than  $r_A$  and  $r_V$  but agreed with  $r_{VA}$ .

## 7. Conclusions

The representation of infinite circular cylinders of ice by equal-V/A spheres works well for all particle sizes, all

wavelengths, and all optical depths. The resulting errors in irradiances and heating rates are smaller than the typical observational uncertainties in measurements of these quantities for natural clouds.

The success of equal-V/A spheres in representing nonspherical particles is closely related to the success found earlier by Hansen and Travis [1974] in representing a size distribution of any shape and width by a monodispersion with the single radius  $r_{\text{eff}}$ , because the V/A ratio of the sphere of radius  $r_{\text{eff}}$  is the same as the ratio of the total volume of the entire size distribution to the total surface area.

The enthusiasm with which the snow-optics community quickly adopted the equal-V/A principle is probably related to the difficulty of defining where one snow grain ends and another begins in a snowpack, since the grains are in contact and often well bonded to each other. Although individual grains cannot be unambiguously identified, the total volume and total surface area in a snowpack are well defined, and methods have been developed to measure them [e.g., Shi et al., 1993]. Representing the snowpack by equal-V/A spheres therefore allows us to define the "grain size" without defining "grain."

Effective radii inferred in remote sensing measurements of ice clouds probably correspond to  $r_{VA}$  rather than to  $r_A$  or  $r_V$ . This may explain why particle dimensions measured in ice clouds and converted to  $r_A$  or  $r_V$  often exceed the particle radii inferred from remote sensing. To characterize the "size" of an ice crystal by a single number, as is often done, the most relevant dimension for radiative properties is not the length but rather the shortest dimension (i.e., the width of a column, the thickness of a plate, or the width of a hollow crystal's wall), since that corresponds most closely to  $r_{VA}$ .

It has been common practice, in publications that put forward accurate computations of scattering by nonspherical particles [e.g., Liou and Takano, 1994; Chylek and Videen, 1994], to compare their results to scattering by equal-volume or equal-area spheres. We argue that in the future all such comparisons should also (or instead) be made to equal-V/A spheres, as Fu and his coworkers have done. Otherwise spheres are not given the opportunity to show how well they can perform.

**Acknowledgments.** We are grateful to B.T.N. Evans for the use of his computer code for randomly oriented infinite cylinders and for generous assistance in making it run properly on our system. We thank Craig Bohren, Qiang Fu, Stefan Kinne, Kuo-Nan Liou, David Mitchell, Piet Stammes, and Warren Wiscombe for helpful discussions, and Andrew Heymsfield for his review of the manuscript. This research was supported by the National Science Foundation under grants OPP-94-21096 and ATM-98-13671.

## References

- Ackerman, S. A., W. L. Smith, J. D. Spinhirne, and H. E. Revercomb, The 27-28 October 1986 FIRE IFO cirrus case study: Spectral properties of cirrus clouds in the 8-12  $\mu\text{m}$  window, *Mon. Weather Rev.*, **118**, 2377-2388, 1990.
- Bohren, C. F., and D. R. Huffman, *Absorption and Scattering of Light by Small Particles*, Wiley, New York, 1983.
- Bryant, F. D., and P. Latimer, Optical efficiencies of large particles of arbitrary shape and orientation, *J. Colloid Interface Sci.*, **30**, 291-304, 1969.
- Chylek, P., and G. Videen, Longwave radiative properties of polydispersed hexagonal ice crystals, *J. Atmos. Sci.*, **51**, 175-190, 1994.
- Dozier, J., Spectral signature of alpine snow cover from the Landsat Thematic Mapper, *Remote Sens. Environ.*, **28**, 9-22, 1989.
- Ebert, E. E., and J. A. Curry, A parameterization of ice cloud optical properties for climate models, *J. Geophys. Res.*, **97**, 3831-3836, 1992.
- Foot, J. S., Some observations of the optical properties of clouds, II, Cirrus, *Q. J. R. Meteorol. Soc.*, **114**, 145-164, 1988.
- Fu, Q., An accurate parameterization of the solar radiative properties of cirrus clouds for climate models, *J. Clim.*, **9**, 2058-2082, 1996.
- Fu, Q., P. Yang, and W. B. Sun, An accurate parameterization of the infrared radiative properties of cirrus clouds for climate models, *J. Clim.*, **11**, 2223-2237, 1998.
- Grenfell, T. C., A radiative transfer model for sea ice with vertical structure variations, *J. Geophys. Res.*, **96**, 16,991-17,001, 1991.
- Grenfell, T. C., and D. K. Perovich, Radiation absorption coefficients of polycrystalline ice from 400 to 1400 nm, *J. Geophys. Res.*, **86**, 7447-7450, 1981.
- Grenfell, T. C., D. K. Perovich, and J. A. Ogren, Spectral albedos of an alpine snowpack, *Cold Reg. Sci. Technol.*, **4**, 121-127, 1981.
- Grenfell, T. C., S. G. Warren, and P. C. Mullen, Reflection of solar radiation by the Antarctic snow surface at ultraviolet, visible, and near-infrared wavelengths, *J. Geophys. Res.*, **99**, 18,669-18,684, 1994.
- Hansen, J. E., and L. D. Travis, Light scattering in planetary atmospheres, *Space Sci. Rev.*, **16**, 527-610, 1974.
- Haracz, R. D., L. D. Cohen, and A. Cohen, Scattering of linearly polarized light from randomly oriented cylinders and spheroids, *J. Appl. Phys.*, **58**, 3322-3327, 1985.
- Heymsfield, A. J., K. M. Miller, and J. D. Spinhirne, The 27-28 October 1986 FIRE IFO cirrus case study: Cloud microstructure, *Mon. Weather Rev.*, **118**, 2313-2328, 1990.
- Kerker, M., *The Scattering of Light and Other Electromagnetic Radiation*, Academic, San Diego, New York, 1969.
- Kinne, S., T. Ackerman, A. Heymsfield, and K. Miller, Radiative transfer in cirrus clouds from airborne flux and microphysical measurements during FIRE-86, in *Seventh Conference on Atmospheric Radiation*, pp. 9-15, Am. Meteorol. Soc., Boston, Mass., 1990.
- Kou, L., D. Labrie, and P. Chylek, Refractive indices of water and ice in the 0.65- to 2.5- $\mu\text{m}$  spectral range, *App. Opt.*, **32**, 3531-3540, 1993.
- Liou, K.-N., Transfer of solar irradiance through cirrus cloud layers, *J. Geophys. Res.*, **78**, 1409-1418, 1973.
- Liou, K.-N., and Y. Takano, Light scattering by nonspherical particles: remote sensing and climatic implications, *Atmos. Res.*, **31**, 271-298, 1994.
- McFarquhar, G. M., and A. J. Heymsfield, The definition and significance of an effective radius for ice clouds, *J. Atmos. Sci.*, **55**, 2039-2052, 1998.
- Mishchenko, M. I., W. B. Rossow, A. Macke, and A. A. Lacis, Sensitivity of cirrus cloud albedo, bidirectional reflectance and optical thickness retrieval accuracy to ice particle shape, *J. Geophys. Res.*, **101**, 16,973-16,985, 1996.
- Mitchell, D. L., and W. P. Arnott, A model predicting the evolution of ice particle size spectra and radiative properties of cirrus clouds, II, Dependence of absorption and extinction on ice crystal morphology, *J. Atmos. Sci.*, **51**, 817-832, 1994.
- Mitchell, D. L., A. Macke, and Y. Liu, Modeling cirrus clouds, II, Treatment of radiative properties, *J. Atmos. Sci.*, **53**, 2967-2988, 1996.
- Perovich, D. K., and J. W. Govoni, Absorption coefficients of ice from 250 to 400 nm, *Geophys. Res. Lett.*, **18**, 1233-1235, 1991.
- Platt, C. M. R., J. D. Spinhirne, and W. D. Hart, Optical and microphysical properties of a cold cirrus cloud: Evidence for regions of small ice particles, *J. Geophys. Res.*, **94**, 11,151-11,164, 1989.
- Pollack, J. B., and J. N. Cuzzi, Scattering by nonspherical particles of size comparable to a wavelength: A new semi-empirical theory and its application to tropospheric aerosols, *J. Atmos. Sci.*, **37**, 868-881, 1980.
- Sassen, K., A. J. Heymsfield, and D. O'C. Starr, Is there a cirrus small particle radiative anomaly?, in *Seventh Conference on Atmospheric Radiation*, pp. J91-J95, Am. Meteorol. Soc., Boston, Mass., J91-J95, 1990.
- Schaaf, J. W., and D. Williams, Optical constants of ice in the infrared, *J. Opt. Soc. Am.*, **63**, 726-732, 1973.
- Schmidt, E. O., R. F. Arduini, B. A. Wielicki, R. S. Stone, and S.-C. Tsay, Considerations for modeling thin cirrus effects via

- brightness temperature differences, *J. Appl. Meteorol.*, *34*, 447-459, 1995.
- Shi, J., R. E. Davis, and J. Dozier, Stereological determination of dry-snow parameters for discrete-scatterer microwave modeling, *Ann. Glaciol.*, *17*, 295-299, 1993.
- Shimizu, H., "Long prism" crystals observed in the precipitation in Antarctica, *J. Meteorol. Soc. Jpn.*, *41*, 305-307, 1963.
- Stephens, G. L., Radiation profiles in extended water clouds, II, Parameterization schemes, *J. Atmos. Sci.*, *35*, 2123-2132, 1978.
- Sun, Z., and K. P. Shine, Parameterization of ice cloud radiative properties and its application to the potential climatic importance of mixed-phase clouds, *J. Clim.*, *8*, 1874-1888, 1995.
- Takano, Y., and K.-N. Liou, Solar radiative transfer in cirrus clouds, I, Single-scattering and optical properties of hexagonal ice crystals, *J. Atmos. Sci.*, *46*, 3-19, 1989.
- Vouk, V., Projected area of convex bodies, *Nature*, *162*, 330-331, 1948.
- Warren, S. G., Optical properties of snow, *Rev. Geophys. Space Phys.*, *20*, 67-89, 1982.
- Warren, S. G., Optical constants of ice from the ultraviolet to the microwave, *Appl. Opt.*, *23*, 1206-1225, 1984.
- Wendling, P., R. Wendling, and H. K. Weickmann, Scattering of solar radiation by hexagonal ice crystals, *Appl. Opt.*, *18*, 2663-2671, 1979.
- Wielicki, B. A., J. T. Suttles, A. J. Heymsfield, R. M. Welch, J. D. Spinhirne, M. L. C. Wu, D.O'C. Starr, L. Parker, and R. F. Arduini, The 27-28 October 1986 FIRE IFO cirrus case study: Comparison of radiative transfer theory with observations by satellite and aircraft, *Mon. Weather Rev.*, *118*, 2356-2376, 1990.
- Wiscombe, W. J., Mie scattering calculations: Advances in technique and fast, vector-speed computer codes, *NCAR Tech. Note TN-140+STR*, Natl. Cent. for Atmos. Phys., Boulder, Colo., 1979.
- Wiscombe, W. J., Improved Mie scattering algorithms, *Appl. Opt.*, *19*, 1505-1509, 1980.
- Wiscombe, W. J., and S. G. Warren, A model for the spectral albedo of snow, I: Pure snow, *J. Atmos. Sci.*, *37*, 2712-2733, 1980.
- Wyser, K., and P. Yang, Average ice crystal size and bulk short-wave single-scattering properties of cirrus clouds, *Atmos. Res.*, *49*, 315-335, 1998.

---

T. C. Grenfell and S. G. Warren, Department of Atmospheric Sciences, Box 351640, University of Washington, Seattle, WA 98195-1640. (tcg@atmos.washington.edu; sgw@atmos.washington.edu.)

(Received January 20, 1999; revised June 16, 1999; accepted June 23, 1999.)